SEMI-ACTIVE DAMPING PERFORMANCE OF IRON PARTICLE FILLED SILICONE RUBBER

Florian Dirisamer[a,*], Umut Cakmak[a], Edmund Marth[b], Zoltan Major[a]

[a] *Institute of Polymer Product Engineering, Johannes Keppler University Linz, Altenbergstraße 69,4040 Linz, Austria*

[b] *Institute of Power Electronics and Electrical Drives, Johannes Keppler University Linz,Altenbergstraße 69, 4040 Linz, Austria*

[*] corresponding author: Florian.Dirisamer@jku.at

ABSTRACT. The aim of this work was to design, produce and evaluate a demonstrator to visualize the magneto-induced damping behaviour of materials. In contrast to standard materials, the damping coefficient of iron particle filled silicone rubbers can be controlled by a semi-active magnetic field. This field effect should be characterized in order to evaluate the suitability of these magnetorheological silicone elastomers for the use in different configurations and applications.

KEYWORDS: semi-active damping, magnetorheological silicone elastomer, damper demonstrator.

1. INTRODUCTION

All products with moving or rotating parts exhibit vibrations in operating state. For most applications these vibrations are unwanted and proper vibration isolation or absorption devices and materials are required to ensure safety and serviceability. Depending on the application (loading, severity of a failure, environmental and operating conditions), vibrations can be reduced by passive (e.g., rubber dampers), semi-active (i.e., adjusting the damping behavior by an external physical field) or active damping (i.e., closed-loop feedback control by inducing counter vibration, among others) [1, 2]

A number of studies [3, 4] have been conducted to understand the magneto-mechanical behavior of silicone rubber filled with magnetically polarizable particles. By applying an external magnetic field, the mechanical behavior is rapidly, continuously and can be reversibly changed. In this work, we investigate the semi-active damping performance of a magnetorheological silicone elastomer. A demonstrator was designed to study the damping performance in varying operating states. The magnetic field is induced directly by the demonstrators electromagnet.

2. CONCEPT AND APPROACH

In order to be able to study as many different O-ring (cross-section) geometries and material formulations as possible and to achieve accurate results, different demonstrator designs were considered. To finally determine the best solution for this task, a so called creative method based morphologic box was used in the conceptual design. For this, the construction of the damper demonstrator was split into three main parts:

- steel case, including an electromagnet
- motor unit
- damping unit
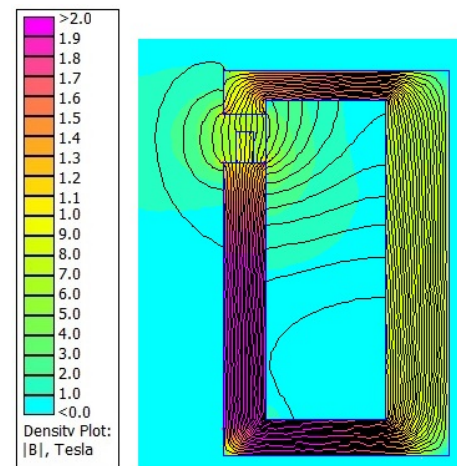
FIGURE 1. Flux density plot of the demonstrator magnet with a coil current density of 10 $A\ mm^{-2}$.

2.1. SIMULATION

A finite element (FE) magnetostatic simulation based on MATLAB and the open source "Finite Element Method Magnetics" (FEMM) software was performed with different geometries of the steel case, since it serves as the iron core of the electromagnet. As the part is rotationally symmetric, it could be represented as a 2D axissymmetric problem. The design was optimized in terms of a space-saving solution and a strong homogeneous field in the air gap, where the damping unit is located. Figure 1 illustrates the simulation result of the final selected geometry.

2.2. CONSTRUCTION AND MANUFACTURING

After designing each of the three main demonstrator parts separately, defining the connections between them the construction could be done in detail. To generate the vibrations, a DC-motor (2342 S018 CR, Faulhaber)
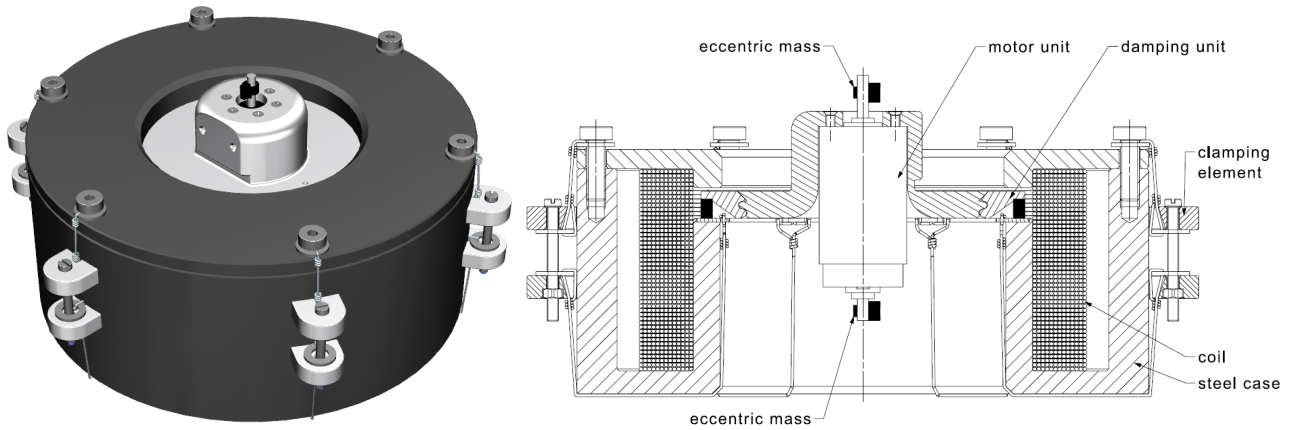
FIGURE 2. Constructed assembly of the Damper demonstrator (left) and damper demonstrator in section view with labelled components(right)

Material	Shore-A hardness
TangoBlack+	27
DM 9860	60
DM 9895	95

TABLE 1. Non-magnetoactive materials used for O-rings

with eccentric weights was used. Figure 2 shows the final construction of the damper demonstrator and its section view.

The motor-mount, the connection-element, some of the tested O-rings and a mold for magnetorheological silicone elastomers were manufactured via a 3D-printing method using photopolymers (Objet Connex 350), the steel case via CNC-turning and -milling and the coil via winding around a zylinder.

3. MANUFACTURING OF THE O-RINGS

In order to show the difference between the damping behaviour of unfilled and iron particle filled silicone rubbers within the magnetic field, O-rings made of different unfilled elastomers and with different contents of iron particles within the silicone rubber were moulded. These materials were glued onto a steel plate to attach them to the steel case and on the connection-element to link it to the motor unit.

3.1. NON-MAGNETOACTIVE

Different photopolymers for 3D-printing (Stratasys Ltd.) were selected as non-magnetoactive materials for the printed O-rings. These materials are one pure TangoBlack+ and two digital materials, mixtures of VeroWhite and TangoBlack+ (Table 1).

3.2. MAGNETOACTIVE

The magnetorheological elastomers were produced from polydimethylsiloxane (PDMS) and mixed with iron particles in the ratios 1:5, 1:10, 1:15 and 1:20. A mold (Figure 3) for manufacturing the O-rings was 3D-printed.
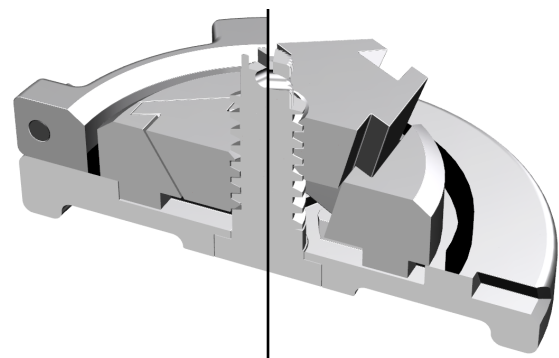
FIGURE 3. Mold in section view - left side with closed outer parts and centerpiece, right side with removed outer parts and collapsed center part.
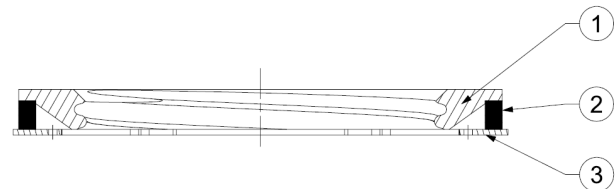
FIGURE 4. Damping unit with labeled components - connection element (1), damping element (2), steel plate (3).

To simplify the demolding, the outer parts can be removed and the centerpiece can be collapsed. The iron powder was dispersed in the PDMS matrix, vacuum was applied to degas the mixture, which was then filled into the mold and finally was cured in the oven for 24 hours at $60°C$. Afterwards these rings were demolded and finally glued to the steel plate and the connection-element (Figure 4).

4. TEST SETUP

To calculate the damping-performance, the acceleration forces in each direction are recorded via an Arduino based acceleration sensor, which is capable of measuring in x, y and z-direction as well as the rotations around these axes. This sensor is placed on the motor unit
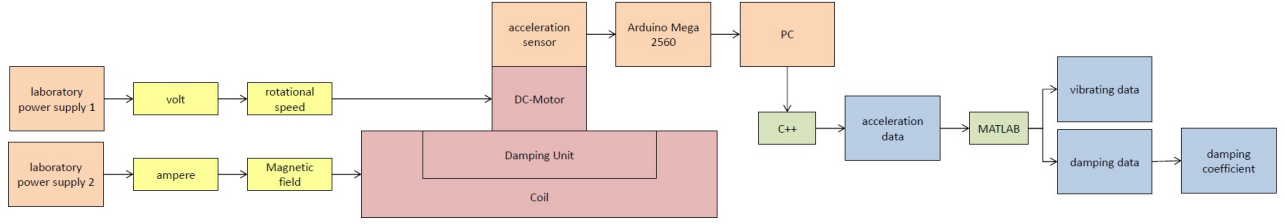
FIGURE 5. Workflow of the Test Setup
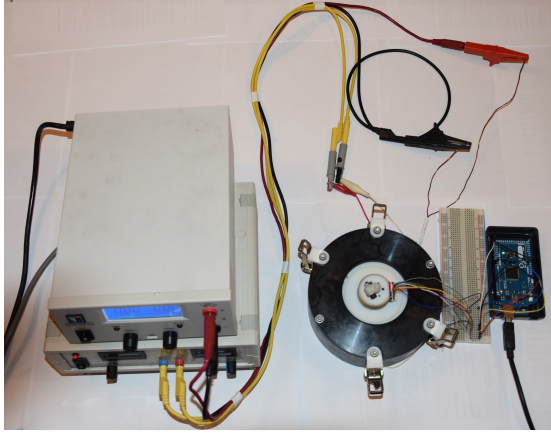
FIGURE 6. Test Setup.

and connected to an Arduino Mega 2560 board, which communicates with the PC, on which a C++ program evaluates the acceleration data to calculate the damping coefficient. The rotational speed of the DC-motor and the magnetic field caused by the coil is driven by two laboratory power supplies. The workflow is shown in Figure 5 and the test setup is shown in Figure 6. The equation for calculating the damping coefficient is given below.

$$d\left(\omega, B\right) = \frac{\sqrt{F_E^2 \cdot \omega^4 - \hat{a}^2\left(B\right) \cdot m_D^2 \cdot \left(\omega^2 - \omega_0^2\right)^2}}{2 \cdot m_D \cdot \hat{a}\left(B\right) \cdot \omega} \tag{1}$$

The parameters F_0, ω_0 and ω are calculated as follows:

$$F_E = m_e \cdot \omega^2 \cdot r_e \tag{2}$$

$$\omega_0 = \sqrt{\frac{k_r}{m_D}} \tag{3}$$

$$k_r = \frac{E}{2 \cdot \left(1 + \nu\right)} \cdot \frac{\pi \cdot D_M \cdot b}{h} \tag{4}$$

$$\omega = 2 \cdot \pi \cdot n \tag{5}$$

The symbols and their physical meanings are listed at the end of this paper.

5. RESULTS

While changing many different configurations of rotational speed of the vibrating motor and the magnetic field of the coil within the damping element, the variation of the acceleration due to the magnetic field for each

damping element could be measured and the damping coefficient (Equation 1) could be calculated. The results are visualized as nominal accelerations, where a decreasing acceleration lead to an increasing acceleration. The rotational speed of the vibrating motor was changed from $0 rpm$ to $8000 rpm$ in 18 steps and the magnetic field within the coil was changed from $0T$ to $0.72T$ in 8 steps.

5.1. NON-MAGNETOACTIVE

Non-magnetoactive materials should not show any influence of the damping coefficient on an incresing coil current. Therefore, the nominal acceleration should be constant. Figure 7 show the result of the non-magnetoactive with an increasing nominal acceleration which indicates an decreasing damping coefficient. This result can be explained via the magnetic field within the steel case, which influence the movement of the DC-Motor.

5.2. MAGNETOACTIVE

The prediction for a magnetorheologic material is, that the damping coefficient will increase with an increasing magnetic field within the damping element. Therefore, the acceleration has to decrease. Figure 8 shows the result for the iron particle filled silicon rubber with an relation of 1:20 at a rotational speed of 2700rpm. The decreasing nominal acceleration for an increasing coil current is clearly to see, apart from the acceleration at $I_{Coil} = 7A$, which can be explained by the same connection as the standard elastomers, the effect of the magnetic field on the movement of the DC-Motor.

6. CONCLUSIONS

This paper compares the influence of the magnetic field on the damping coefficient of magnetorheologic and non-magnetorheologic materials. Therefore, this demonstrator was designed to visualize these effects. In general, the result of an increasing damping coefficient for magnetorheologic materials with an increasing magnetic field within the damping element are shown. However these predicted progresses are superimposed by a second progress, which can be interpreted as the influence of the magnetic field within the center of the steel case, which affects the movement of the DC-Motor. As a result, the damping coefficient of the non-magnetorheologic material seems to decrease, which is not possible for that material.
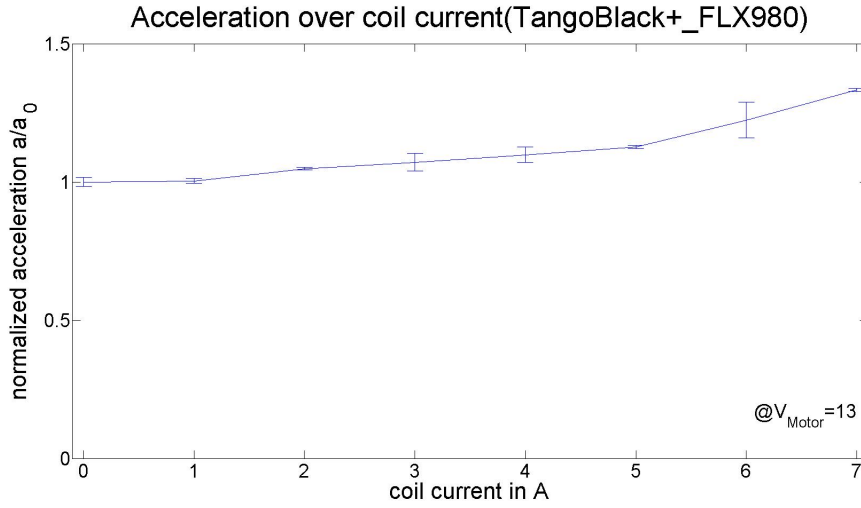
FIGURE 7. Results - standard material.
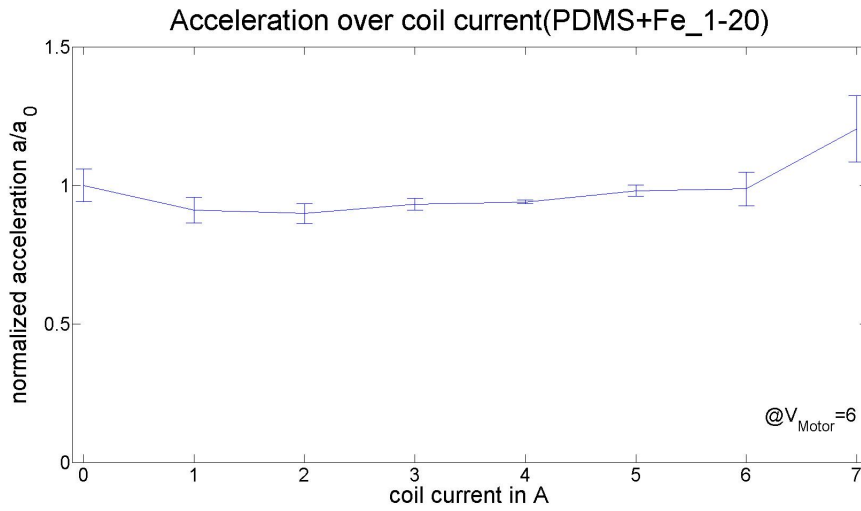
FIGURE 8. Results - iron particle filled silicone rubber.

LIST OF SYMBOLS

$\hat{a}$ maximum acceleration $[\mathrm{m\,s}^{-2}]$

B magnetic field $[\mathrm{T}]$

b width damping element $[\mathrm{m}]$

d damping coefficient $[\mathrm{N\,s\,m}^{-1}]$

D_M mean diameter damping element $[\mathrm{m}]$

E Young's modulus $[\mathrm{MPa}]$

F_E Force of eccentric mass $[\mathrm{N}]$

h height diameter damping element $[\mathrm{m}]$

k_r spring constant $[\mathrm{N\,m}^{-1}]$

m_D mass damping and motor unit $[\mathrm{kg}]$

m_e mass eccentric mass $[\mathrm{kg}]$

ν Poisson's ratio $[-]$

n rotational speed $[\mathrm{s}^{-1}]$

r_e distance center of mass to axis of rotation $[\mathrm{m}]$

ω angular frequency $[\mathrm{rad\,s}^{-1}]$

ω_0 characteristic angular frequency $[\mathrm{rad\,s}^{-1}]$

REFERENCES

[1] D. Sciulli. Dynamics and control for vibration isolation design 1997.

[2] U. Çakmak, F. Hiptmair, Z. Major. Applicability of elastomer time-dependent behavior in dynamic mechanical damping systems. *Mechanics of Time-Dependent Materials* **18**(1):139–151, 2014. DOI:10.1007/s11043-013-9219-z.

[3] M. Lokander, B. Stenberg. Performance of isotropic magnetorheological rubber materials. *Polymer Testing* **22**(3):245–251, 2003. DOI:10.1016/S0142-9418(02)00043-0.

[4] Z. Major, B. Schrittesser, G. Filipcsei. Characterisation of dynamic mechanical behaviour of magnetoelastomers. *Plastics, Rubber and Composites* **38**(8):313–320, 2009. DOI:10.1179/146580109X12473409436986.